

Received December 2, 2020, accepted December 16, 2020, date of publication January 4, 2021, date of current version March 5, 2021.

Digital Object Identifier 10.1109/ACCESS.2020.3048940

Optimal Protection Coordination Scheme for Radial Distribution Network Considering ON/OFF-Grid

MUHAMMAD USAMA^{1,2}, MAHMOUD MOGHAVEMI^{1,3},
HAZLIE MOKHLIS¹, (Senior Member, IEEE),
NURULAFIQAH NADZIRAH MANSOR¹, (Member, IEEE), HAROON FAROOQ²,
AND ALIREZA POURDARYAEI^{1,4}

¹Department of Electrical Engineering, Faculty of Engineering, University of Malaya, Kuala Lumpur 50603, Malaysia

²Department of Electrical Engineering, Rachna College of Engineering and Technology (A Constituent College of University of Engineering and Technology, Lahore), Gujranwala 52250, Pakistan

³Department of Electrical Engineering, University of Science and Culture, Tehran 1461968151, Iran

⁴Department of Electrical and Computer Engineering, University of Hormozgan, Bandar Abbas 7916193145, Iran

Corresponding author: Nurulafiqah Nadzirah Mansor (afiqah.mansor@um.edu.my)

This work was supported by the University of Malaya (UM) under Faculty Research Grant GPF059A-2018 and Grant GPF045A-2019.

ABSTRACT Technology advancement for renewable energy resources and its integration to the distribution network (DN) has garnered substantial interest in the last few decades. Integrating such resources has proven to reduce power losses and improve the reliability of DN. However, the growing number of these resources in DN has imposed additional operational and control issues in voltage regulation, system stability, and protection coordination. Incorporation of various types of distributed generators (DG) into DN causes significant changes in the system. These including new fault current sources, new fault levels, a blinding effect in the protection scheme, reduction in the reach of relays, and decrement in the detection of low-level fault currents for existing relays. Such changes will jeopardize the effectiveness of the entire protection scheme in the DN. This research aims to propose a robust protection scheme in which the relay coordination settings are optimized based on the network layout. The potential impacts of DGs on the DN are mitigated by utilizing a user-defined overcurrent-based relay characteristic to obtain the minimum operating time while satisfying protection coordination constraints. A hybrid optimization algorithm based on Metaheuristic and Linear Programming that has the capability to attain the optimal solution and reduces computational time is proposed in this work. The performance of the proposed technique is tested on radial DN integrated with microgrid (MG). The results obtained show the proposed technique has successfully reduced the relay operating time while meeting the protection coordination requirements for dynamic operating modes of a network.

INDEX TERMS Directional overcurrent relay (DOCR), hybrid optimization, microgrids (MG), protection coordination scheme, user-defined relay characteristics.

NOMENCLATURE

TMS	Time multiplier setting	t_{bk}^f	Operating time of the backup relay
PCS	Pickup current setting	I_{PUBi}	Pickup current upper bound limit value
SC	Standard characteristics	PSM	Plug setting multiplier
NSC	Non-standard characteristics	TCC	Time-Curve Characteristic
UDC	User-defined characteristics	SSA	Salp Swarm Algorithm
TMS_i	Time multiplier setting corresponding to relay i	LP	Linear programming
CTI	Coordination time interval	n	Dimension of search space
t_p^f	Operating time of the primary relay	PCS_i	Pickup current setting corresponding to relay i
		i	Number of relays
		A_i	Time characteristics constant of i^{th} relay
		B_i	Time characteristics constant i^{th} relay
		f	Fault location at the midpoint of a line

The associate editor coordinating the review of this manuscript and approving it for publication was Bin Zhou¹.

- t_i Operating time of the relay
- X^1 Position of Leading Salp
- X_j^i Position of Follower Salps
- Y_i Position of the food source (fitness function)
- I_{PLBi} Pickup current lower bound limit value
- A_{UBi} Relay constant A upper bound limit
- A_{LBi} Relay constant A lower bound limit
- B_{UBi} Relay constant B upper bound limit
- B_{LBi} Relay constant B lower bound limit
- c_1, c_2, c_3 Randomly assigned numbers

I. INTRODUCTION

Increasing concerns on environmental pollution and global warming caused by greenhouse gases generated by conventional energy (e.g. fossil fuels) have developed a significant interest in research and development of renewable energy resources (RES). In recent years, the integration of RES such as wind and solar energy in the MW range into distribution networks (DN) has accelerated with on-site generation near consumption points. However, the integration of such distributed resources changes the existing network topology. In case of abnormal network conditions, the protection scheme might malfunction and result in an uncontrollable operation of the system. In this regard, IEEE standard 1547–2003 has specified the requirements on the RES units to stop injecting power into the DN when the system is de-energized due to faults [1], [2].

The concept of microgrid (MG) was devised for a deliberate and controlled operation of integrated networks as one of the solutions to alleviate the technical issues concerning the high penetration of DG units in the system [3]. The most important benefit of MG is to provide reliable and high-quality power for consumers who require uninterruptible power supplies. Despite numerous advantages provided by MGs, some technical challenges are required to be met, such as MG protection and its entities. Conventional DN protection devices are normally designed according to the large fault currents, and thus they cannot protect MGs when it operates in the islanded mode. This is due to the DGs based on inverter-type cannot contribute an adequate current towards the total fault current when a fault occurs in the MG [4], [5]. In addition, high DG penetration into the DN creates a new source of fault currents, which in turn increases the short circuit levels, alters the current magnitude, and causes the bidirectional tripping of protection relays might occur, leading to maloperation and loss of coordination of the entire protection scheme in the network. Furthermore, different DG types and their capacities contribute diverse fault current levels in MG that might further degrade the protection relay coordination [8]. Therefore, the conventional protection scheme requires improvements and modifications to address the challenges highlighted previously caused by the inevitable connection of DGs in the existing DN.

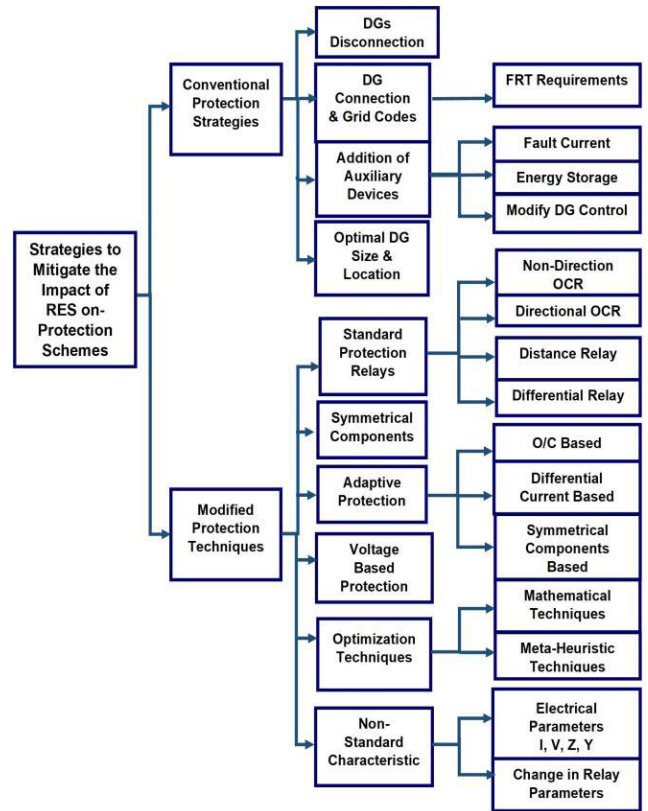


FIGURE 1. Protection strategies for interconnected Distribution Networks.

Substantial literature is available on conventional and modified protection techniques to provide an adequate protection strategy for renewable integrated power networks. The authors in [9]–[11] summarized the various approaches and coordination schemes for the protection system based on additional components and user-defined characteristics required for the stable operation of the network, as illustrated in Fig. 1. Moreover, references [12]–[14] highlighted the protection coordination challenges in DN with high penetration of DGs and MGs. Several solutions have been proposed based on analytical techniques, optimization methods, and adaptive protection schemes to mitigate the protection coordination challenges resulted from vast new DG connections to DN. Some authors have reported devising a new protection solution based on the amendment in protection standard characteristics in recent years. Study in [15] provides a comprehensive analysis of the non-standard characteristics (NSC) in which the proposed work shows a promising solution to mitigate the relay coordination issues.

Relay coordination study requires a proper adjustment and coordination of pickup current and time dial settings. Several studies have been conducted on this in the past by manipulating the standard characteristics (SC) parameters rather than pickup current (PCS) and time multiplier (TMS) settings [15]–[18]. The protection coordination is a nonlinear, non-convex, and highly constrained problem in nature. Thus, various analytical and optimization

algorithms have been explored to coordinate the primary and backup relays. Analytical methods are considered useful techniques for radial distribution networks; however, for large meshed networks, it requires substantial computational time to determine the optimal relay settings. Other approaches available for relay coordination, includes Linear Programming (LP) [19], Mixed-integer Non-Linear Programming (MINLP) [20], Non-linear Programming (NLP) [21], and heuristic-based algorithms [22], [23]. These approaches manage to obtain optimal relay settings in a shorter time compared to analytical methods. In particular, heuristic and meta-heuristic algorithms are known to have a wider search space to generate several populations to get the best global optimum solution. In this regard, many optimization techniques have been proposed in [24], [25] to optimize the relay coordination settings, such as Genetic Algorithm (GA), Particle Swarm Optimization (PSO), Ant-Colony Optimization (ACO), and Cuckoo Search (CS) algorithm. Although meta-heuristic techniques are capable of finding a global solution, however, for a large-scale integrated network, relay coordination has become a highly constrained problem. Therefore, there is a high probability of an infeasible solution generated during the searching process. Consequently, the process of updating these infeasible solutions may converge to a local optimum. Therefore, hybrid optimization techniques have been proposed in the literature [26]–[28] to overcome this issue for highly constrained protection problems.

A robust hybrid optimization framework for active distribution networks (ADN) has been proposed in [27], [29]. The authors considered network uncertainties and topological changes, e.g. changes in network operating modes and fault conditions, measuring error in equipment, and DG outage. The author in [27] has obtained the optimal protection settings for MG, considering all the topological changes using Genetic and Linear Programming (GA-LP) optimization technique. In [29], a two-steps hybrid optimization algorithm consisting of Cuckoo Search-Linear Programming (CS-LP) for relay constants (A, B, PCS, and TMS) provides adequate coordination intervals in primary and backup relays for MG during the various operating conditions. Utilizing the benefits of Non-standard characteristics, the work in [30] has proposed a robust protection coordination scheme for meshed networks by implementing dual settings of DOCR. A remarkable reduction of relays total operating time was achieved by introducing non-standard inverse-time characteristics that can be explicitly applied in numerical relays. Considering the complexity and controllability of relays in ADN, a user-defined microprocessor-based DOCR protection scheme is implemented in [31], where the scaling factor is employed for each relay to alleviate the complexity of the relay coordination process for the far end faults. The proposed logic utilized a user-defined relay coordination strategy to reduce the total tripping time of relays in grid-connected and islanding operating modes. However, the difficulty arises with the change in network configuration and layout with respect to future planning. Furthermore, the active network

management (ANM) approaches, such as network reconfiguration (NR) and demand response have introduced challenges to modern DN-based MG protection settings. The NR approach is utilized to minimize power losses and maintain the load demand. However, this leads to a complex protection coordination scheme. Many adaptive techniques have been proposed in the literature to update the protection settings considering the pre-contingency network state (prior to a fault occurrence). The schemes for fault recovery of MG have been discussed to detect permanent faults and change in network topologies [32]–[34].

Although some of the discussed approaches suit well to find the optimal relay settings during network changes, these protection schemes do not provide efficient protection against the faults originating after a change in MG status (on/off-grid), grid reconfiguration, and division of the grid into multiple operating zones after a permanent fault. Therefore, by utilizing the benefits of programmable numerical relays, this paper proposes a fast hybrid optimization technique that combines the Salp-Swarm Algorithm (SSA) with Linear Programming (LP) (SSA-LP). In this approach, the protection coordination problem (PCP) is optimized for relay coordination using standard and user-defined characteristics. Moreover, a constrained mathematical model designed for service restoration of radial DN with integrated DGs is also employed in grid-connected and islanded modes. The electrical boundaries of islands, along with current directions and magnitudes, are obtained from the service restoration model. Based on the restored network, new fault current values are estimated, and the proposed hybrid technique is utilized to acquire the updated relay settings to achieve coordination for both pre- and post-contingency faults. The main contributions of this paper are as follows:

- Optimal protection coordination settings using a fast hybrid optimization technique for the DN integrated with MG.
- A comparative analysis to obtain minimum operating time for the DOCR coordination using the standard and user-defined characteristics.
- Optimal relay coordination settings to provide fast operation of protection devices during post contingency faults in reconfigured MGs.

The rest of the paper is organized as follows: Section II briefly discusses the challenges of protection in interconnected DN. Section III presents the protection coordination problem formulation, while section IV explains the proposed hybrid SSA-LP optimization technique. Section V presents simulation results conducted on 9-Bus Canadian radial DN and 23-Bus Malaysian radial DN to verify the efficiency of the proposed method for different network operating scenarios. Section VI gives the conclusion of the conducted research.

II. PROTECTION COORDINATION CHALLENGES IN INTERCONNECTED DISTRIBUTION NETWORKS

MG integration into the network has enhanced the grid reliability, provided backup during utility outages, reduced

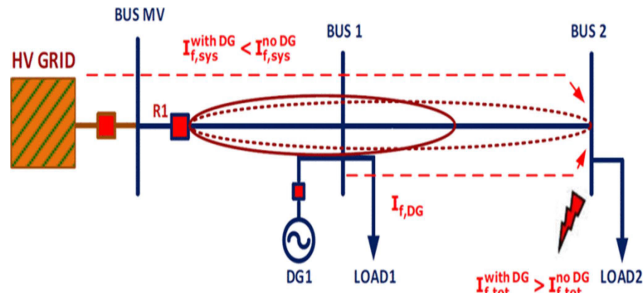


FIGURE 2. Fault current contribution in case of protection blinding [38].

power losses, improved voltage profile, and increased grid efficiency during peak load demand. Despite various advantages of MG, some technical challenges arise with the connection of MGs in the DN. Such embedded novel topologies and integration have caused the protection coordination challenges that could cause maloperation of the network. In [10], [35], [36], some DG technologies such as Synchronous based DGs generally inject high fault currents in the range of 5-6 times of nominal rated current, which cause significant changes in fault current level. Other technologies like inverter interfaced DGs (IIDG) contribute 1.1–3 times the rated current towards the total fault current. It is because the inverters have a low thermal overload capability, limiting their maximum output fault current [10],[35]–[37].

With the intervention of a multiloop system in the interconnected DN, the direction power flow does not remain unidirectional as considered in passive conventional distribution networks; hence the fault direction changes according to the fault location. The incorporation of active DGs on a large scale creates the new fault current sources, which increases the short circuit levels, alters the current magnitude, and causes the bidirectional current. Consequently, the upstream relays underreach the fault current and jeopardize the feeder relay sensitivity based on the fault location; thus, the downstream relays get trip and lead to maloperation, termed as protection blinding, as shown in Fig. 2 [38].

Another issue relates to the Nuisance Tripping or False tripping of the relays. The adjacent healthy feeder’s relay gets trip earlier than the faulty feeder relay because of bidirectional current flow. Fig. 3 shows that without a DG connection, the fault current is only catered by the grid. But, with the integration of DG, there may be the case that non-directional overcurrent R₁ sends the trip command to its associated circuit breaker earlier than the forward operation of R₂, which may trip the healthy feeder-1 instead of the faulted feeder. This kind of tripping can also create unwanted islanding with its connected load and may lead to unsafe operation of the network.

Other kinds of problems like cascade failure of the relay because of loss of coordination, unintentional islanding due to fault at grid or substation, auto reclosure at faulted bus because of fault currents injected by DGs in some cases are all categorized as protection coordination

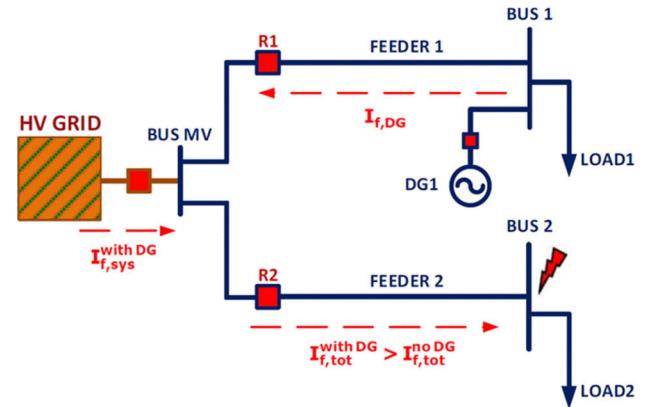


FIGURE 3. Fault current contribution in case Nuisance Tripping [38].

TABLE 1. IEC 60255 Standard Relay Constants for Overcurrent.

Curve Type	A	B
Standard Inverse (IDMT)	0.14	0.02
Very Inverse (VIN)	13.5	1
Extremely Inverse (EI)	80	2
Long Inverse Standard Inverse (LI)	120	1

problems [10], [38], [39]. Considering all the sensitivity and selectivity issues of line protection, an efficient and reliable protection scheme needs to be provided for the stable operation of interconnected networks during different grid scenarios and fault conditions. If a fault occurs on the utility grid, the desired response is to isolate MG from the rest of the network. This leads to the autonomous operation of MG, and if a fault takes place within the MG, the protection system should remove the smallest possible faulted area of MG to clear the fault.

III. PROPOSED FORMULATION FOR PROTECTION COORDINATION PROBLEM

In this study, IEC (International Electrotechnical Commission) 60255 standard characteristics are considered for relay coordination purposes with the relay characteristic constants specified in Table 1 [40]. The operating time equation of a standard inverse definite minimum time (IDMT) over current is given in Eq. (1) below:

$$T_{op} = \frac{A * TMS}{\left(\frac{I_{sc}}{CTR * I_p}\right)^2} \quad (1)$$

whereas T_{op} is the operating time of the relay, TMS is the time multiplier setting; I_{sc} is the short circuit current flows from the relay coil. CTR is the relay current transformation ratio, and I_p is the Pickup current tap setting of the relay. Further, the product of CTR and I_p is termed as Pickup current setting (PCS), which determines the current level at which the relay operates. Whereas A and B are the relay characteristic constants as specified in Table 1.

TABLE 2. Optimization result of relay settings for scenario-1(grid-connected) for 9-bus radial DN.

Relays	Standard Characteristics						User-Defined Characteristics							
	GA_LP [27]		CS_LP [29]		Proposed SSA_LP		CS_LP [29]				Proposed SSA_LP			
	PCS	TMS	PCS	TMS	PCS	TMS	PCS	TMS	A	B	PCS	TMS	A	B
1	0.5	0.309	2.5	0.359	2.5	0.250	2.5	1.662	12.5	1	2.3	0.214	9.06	0.4
2	2	0.068	2.5	0.337	2.5	0.05	2.5	1.003	9.07	1	1.8	0.05	0.14	0.99
3	0.6	0.205	2.5	0.247	2	0.213	2.5	1.295	9.44	1	2.5	0.168	13.12	1
4	2.5	0.054	2.5	0.434	2	0.101	2.5	1.054	13.5	1	1.1	0.159	9.94	1
5	1	0.1	2.5	0.146	1.8	0.108	2.5	0.717	9	1	1.5	0.101	8.9	0.56
6	2.5	0.06	2.5	0.541	1.9	0.151	2.5	2.578	8.3	1	1.3	0.183	7.32	0.76
7	0.5	0.05	0.5	0.1	0.5	0.05	2.5	0.1	11.6	0.64	2.11	0.05	0.14	0.41
8	1.5	0.05	2	0.561	0.5	0.400	0.5	0.72	11.6	0.56	1.5	0.206	8.32	0.8
9	2.5	0.139	2.5	0.346	0.8	0.302	2.5	1.34	12.5	1	1.5	0.262	4.73	0.5
10	2.5	0.05	2.5	0.388	2.5	0.05	2.5	1.263	11.8	1	0.6	0.05	0.14	0.63
11	2.5	0.108	2.5	0.275	1.5	0.209	2.5	1.196	13.5	1	2.4	0.139	13.49	0.82
12	1	0.092	2.5	0.363	2.2	0.101	2.5	0.656	12.5	1	2.35	0.127	12.55	1
13	2.5	0.064	2.5	0.165	2	0.120	2.5	1.152	7.11	1	1.95	0.107	3.82	0.91
14	1	0.111	2.5	0.452	1.1	0.176	2.5	0.592	13.5	1	1.04	0.169	4.61	0.79
15	0.5	0.05	2.5	0.1	0.5	0.05	2.5	0.1	11.9	0.76	0.75	0.05	5.13	0.99
16	1.5	0.05	2.5	0.577	2.5	0.202	1.2	2.915	3.18	0.67	0.80	0.210	11.61	0.96
OF	11.239 sec		18.175 sec		5.443 sec		10.9324 sec				3.650 sec			

The objective of the work is to minimize the total operating time for primary relays for the faults on lines to maintain selectively and coordination between the near end and far-end relays. Moreover, the reduction in the primary relay operating time led to a reduction in backup operating time as well if they are properly coordinated. The objective function (OF) is defined by Eq. (2).

$$OF = \min T = \sum_{i=1}^N t_i \tag{2}$$

where N is the total number of relays, and t_i is the operating time of the near end and far end relay. To solve the PCP, a set of relay constraints must be defined for optimization purposes. The conventional relay settings normally have two sets of constraints expressed in Eq. (3) and (4). While for proposed work, another allowed range for relay variables are mentioned in Eqs. (5) to (6).

$$TMS_{i_min} < TMS_i < TMS_{i_max} \quad \forall i = 1, 2, \dots, N \tag{3}$$

$$PCS_{i_min} < PCS_i < PCS_{i_max} \quad \forall i = 1, 2, \dots, N \tag{4}$$

$$A_{i_min} < A_i < A_{i_max} \quad \forall i = 1, 2, \dots, N \tag{5}$$

$$B_{i_min} < B_i < B_{i_max} \quad \forall i = 1, 2, \dots, N \tag{6}$$

The time dial value is taken as a continuous range, and the value set for lower and upper TMS is between 0.05-1.1. The minimum bound for pickup current is set as twice of rated load value for the relay current settings, whereas for maximum setting, it is taken as 1/3 of the minimum fault value [41], [42]. Therefore, in this work, the PCS value

is assumed as discrete in the range of 0.5-2.5. The values for standard IEC normal inverse relay characteristic curve constant, A & B are 0.14 & 0.02, as mentioned in Table 1. For the proposed user-defined curve, the A&B parameters are selected from 0.14 to 13.5 and 0.02 to 1, respectively. These values have been selected based on the IEC standard 60255 relay characteristics, i.e., Normal Inverse and Very Inverse time-current relay characteristics [17, 31]. As a result, the proposed relay curve can provide better optimal settings and improve the overall relay performance.

A set of constraints must be defined to ensure the selectivity between relays, generally known as a coordination time interval (CTI). This time interval ensures a safe operation for primary and backup relays. CTI is usually set according to industrial and IEEE 242-2001 standards in between 200msec to 500msec [27], [40], [43]. For reliable relay operation, the CTI is selected as 200msec in Eq. (7) based on relay errors, circuit breakers tripping time and the safety margins.

$$t_{bkj}^f - t_{pj}^f \geq CTI \quad \forall f, [k, j] \tag{7}$$

$$t_{min} < t_i < t_{max} \quad \forall i = 1, 2, \dots, N \tag{8}$$

$$t_{imin} \geq 0.05 \quad \forall i = 1, 2, \dots, N \tag{9}$$

The subscript p in Eq. (7) represents the primary relay, while the bk shows its respective backup relay. The variables t_{pj} and t_{bkj} represent the primary and backup relay operating for the fault location at line j when ‘f’ topology is considered. The t_{min} and t_{max} in Eq. (8) shows the time bound for the minimum and maximum operating time of primary relays.

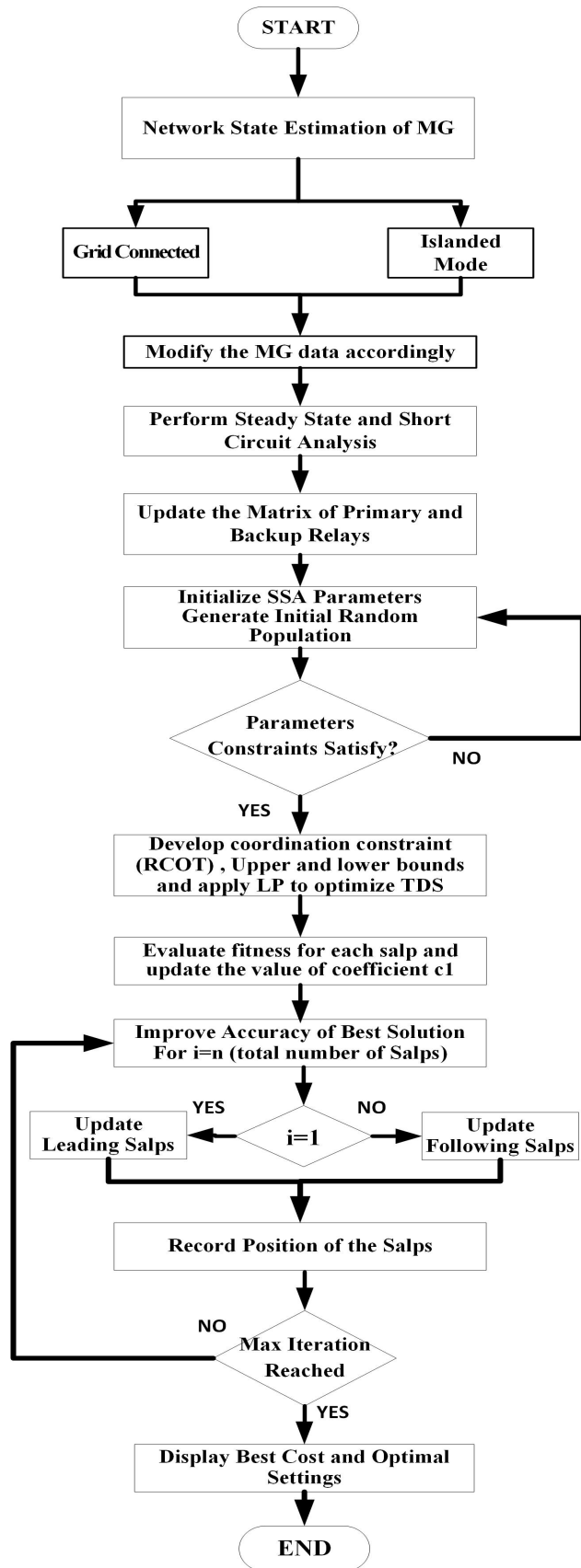


FIGURE 4. Flow chart for the proposed Hybrid Optimization Technique.

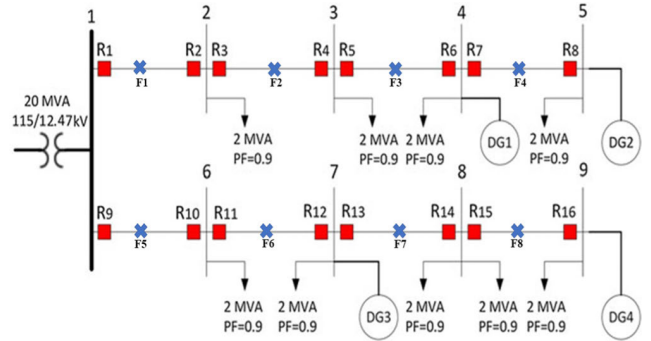


FIGURE 5. Radial 9-Bus Interconnected Distribution Network.

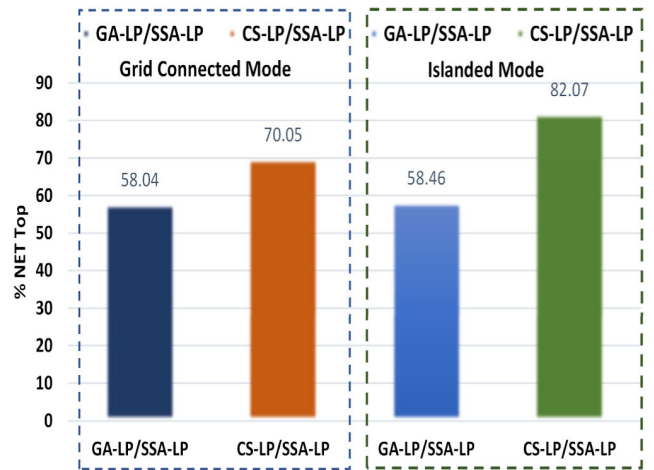


FIGURE 6. Percentage relay operating time of the SSA-LP with the established hybrid techniques for 9-bus radial networks.

IV. PROPOSED METHODOLOGY

In this research, the complexity of the relay coordination problem is reduced through the linearization of the coordination problem. The proposed hybrid optimization approach is based on Salp-Swarm Algorithm & Linear Programming (SSA-LP) attains optimal relay coordination settings for both pre contingency and post contingency fault scenarios. This SSA-LP algorithm minimizes the total operating time of relays in two integrated phases. The first phase uses the SSA method to find the possible relay settings (I_{pu} , A , and B) from ‘n’ dimensional search space for the initial population, defined in Eq. (10-11). The second phase uses a linear programming approach to obtain the optimal TMS value based on relay settings attained from the first phase. After the initialization phase, like other metaheuristics techniques such as GA and PSO, the SSA algorithm selects the best fitness value as the position of leading salp (X^1) from the initial exploring process of search space. The best population in SSA never wipe out even the current population deteriorates after updation; it only updates when SSA finds a better population than the previous one.

TABLE 3. Optimization result of relay settings for scenario-2(islanding) for 9-bus radial DN.

Relays	Standard Characteristics						User-Defined Characteristics							
	GA_LP [27]		CS_LP [29]		Proposed SSA_LP		CS_LP [29]				Proposed SSA_LP			
	PCS	TMS	PCS	TMS	PCS	TMS	PCS	TMS	A	B	PCS	TMS	A	B
1	2	0.409	2.5	0.29	1.1	0.149	2.5	0.964	9.63	1	1.1	0.219	0.8	0.27
2	2.5	0.235	2.5	0.298	2.1	0.09	2.5	0.497	13.05	1	0.9	0.05	0.8	0.78
3	1	0.442	2.5	0.203	0.8	0.125	2.5	2.363	2.43	1	0.7	0.157	4.67	0.59
4	2.5	0.415	2.5	0.375	2.5	0.125	2.5	0.694	13.03	1	1.2	0.129	7.72	0.98
5	0.8	0.484	2.5	0.127	0.5	0.097	2.5	0.612	5.29	1	0.56	0.097	6.44	0.23
6	1.5	0.42	1.5	0.545	2.2	0.175	1	1.180	11.65	0.78	1.5	0.142	3.66	0.35
7	0.6	0.623	0.5	0.1	0.5	0.05	0.5	0.1	2.28	0.24	1.1	0.05	0.14	0.8
8	2.5	0.329	0.5	0.873	1.5	0.198	0.5	0.727	0.14	0.02	2	0.055	5.94	0.11
9	1	0.424	2.5	0.300	0.7	0.170	2.5	1.134	8.61	1	0.7	0.182	10.71	0.79
10	2.5	0.228	2.5	0.327	2.1	0.099	0.5	0.992	0.59	0.16	2.5	0.05	0.14	0.97
11	2	0.341	0.5	0.354	0.5	0.129	1.9	0.136	10.70	0.64	0.64	0.129	0.24	0.02
12	2.5	0.501	0.5	2.029	2.5	0.126	2	2.741	3.17	1	1.9	0.135	7.85	1
13	1	0.715	2.5	0.138	0.8	0.103	2.5	0.737	5.31	1	0.8	0.101	4.16	0.89
14	2.5	0.56	1.1	1.708	1.1	0.164	2.5	1.800	4.70	0.98	2	0.143	7.88	0.59
15	2.5	0.342	0.5	0.1	0.5	0.05	1.1	0.1	8.38	0.64	0.5	0.05	12.29	1
16	1	0.388	2.4	1.382	1.3	0.203	1.4	0.160	3.75	0.15	2.31	0.800	1.42	0.51
OF	14.105 sec		32.3871 sec		5.859 sec		14.7147 sec				4.341 sec			

TABLE 4. CT ratio of relays for 23-bus network.

Relay #	CTR	Relay #	CTR	Relay #	CTR
1	150/5	13	50/5	25	150/5
2	150/5	14	100/5	26	150/5
3	200/5	15	100/5	27	150/5
4	200/5	16	50/5	28	200/5
5	200/5	17	50/5	29	200/5
6	200/5	18	150/5	30	100/5
7	200/5	19	150/5	31	50/5
8	200/5	20	100/5	32	50/5
9	200/5	21	100/5	33	50/5
10	250/5	22	100/5	34	100/5
11	50/5	23	100/5	35	100/5
12	50/5	24	150/5		

For the standard characteristic curve:

$$X_i^{1:n} = rand(\dots) [I_{pUBi} - I_{pLBi}] + I_{pLBi} \quad \forall i \in \text{no. of variables} \quad (10)$$

For the non-standard characteristic curve

$$X_i^{1:n} = rand(\dots) [(I_{pUBi} - I_{pLBi}) + I_{pLBi} (A_{UBi} - A_{LBi}) + A_{LBi} (B_{UBi} - B_{LBi}) + B_{LBi}] \quad \forall j \in \text{no. of variables} \quad (11)$$

Unlike other metaheuristic techniques, the SSA updates the position of follower salps, according to Eqn. (12-13). The follower slap updates their position with respect to each other to let them move towards the leading salp (X^1) gradually. The gradual movements of follower salps

(X_j^i) prevent the SSA from easily stagnating into local optima. These solutions further determine the promising areas of search space to avoid local stagnation termed as exploitation. These updated solutions move gradually

TABLE 5. Load data for 23-bus Malaysian distribution network.

Bus #	Connected Load		Load Condition
	MW	MVAR	
3	0.110	0.070	Non-Critical
4	0.430	0.270	Non-Critical
5	0.100	0.050	Non-Critical
6	0.026	0.017	Non-Critical
7	1.250	0.940	Critical
8	0.130	0.050	Semi-Critical
9	0.340	0.170	Semi Critical
10	0.500	0.02	Semi Critical
11	0.230	0.160	Non-Critical
12	0.250	0.140	Non-Critical
13	0.180	0.110	Non-Critical
14	0.300	0.180	Non-Critical
15	0.160	0.110	Non-Critical
16	0.260	0.170	Non-Critical
17	0.220	0.130	Semi-Critical
18	0.390	0.260	Critical
19	0.200	0.130	Semi-Critical
20	0.270	0.140	Non-Critical
21	0.210	0.110	Critical
22	0.140	0.080	Non-Critical
23	0.110	0.050	Non-Critical

towards the optimal solution and improve the quality of current populations.

Furthermore, SSA has only one main controlling parameter c_1 , which reduces the complexity of the algorithm. It decreases with the increase of iteration, which helps the algorithm to explore the search space at the starting and exploits it at the ending phase. Its simple mathematical model expressed in (14) makes this technique easy to implement to solve optimization problems compared to other established techniques as given in [44]. The detailed steps of the proposed approach are illustrated in Fig. 4.

$$c_1 = 2e^{-\left(\frac{it}{T}\right)^2} \quad (12)$$

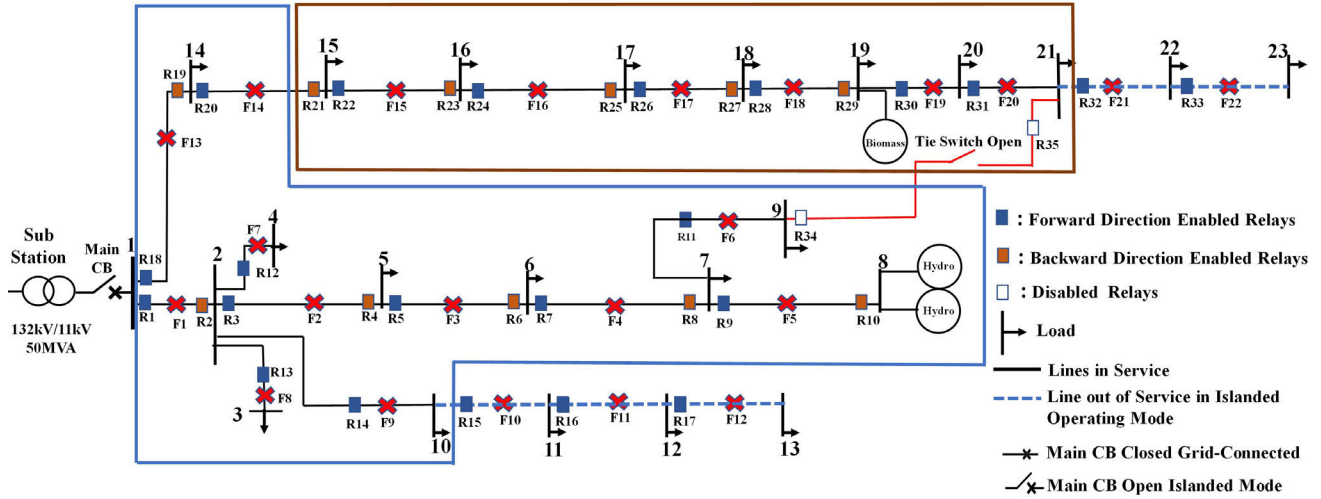


FIGURE 7. 23-Bus Malaysian Radial Distribution Network Interconnected with MG based DG units.

$$X_j^i = \frac{1}{2}at^2 + v_0t \quad (13)$$

whereas c_1 , c_2 , and c_3 are the randomly assigned numbers in the range of 0 to 1.

$$X_j^1 = \begin{cases} Y_i + c_1 ((UB_j - LB_j) c_2 + LB_j) c_3 \geq 0 \\ Y_i - c_1 ((UB_j - LB_j) c_2 + LB_j) c_3 < 0 \end{cases} \quad (14)$$

V. SYSTEM DETAILS AND SIMULATION RESULTS

This section presents a proposed hybrid optimization technique (SSA-LP) to solve the relay coordination problem in an interconnected radial DN. This section also illustrates the description of test models under study. The simulation results have been carried out on the test models in MATLAB software by considering different relay characteristics parameters.

Finally, the optimized relay settings obtained by the proposed algorithm are implemented on ETAP software (version 19.0.1) to verify the coordination settings between relays during fault conditions. The network comprises ALSTOM (P139) model directional and non-directional overcurrent relays with their associated coordination primary and backup relay pair. The following scenarios have been considered to evaluate the performance of the hybrid optimization approach on both test networks.

Scenario 1: The system in grid-connected mode.

Scenario 2: The system is in islanded mode.

Scenario 3: The system is reconfigured following fault scenarios.

A. 9-BUS CANADIAN SYSTEM

The one-line diagram for the 9-Bus Canadian benchmark power distribution network is shown in Fig. 5 [27], [29], [45]. The test system is fed with a 500MVA short circuit capacity grid and X/R ratio of 6%. The utility grid is connected through a 115 kV/12.47 kV substation transformer with a

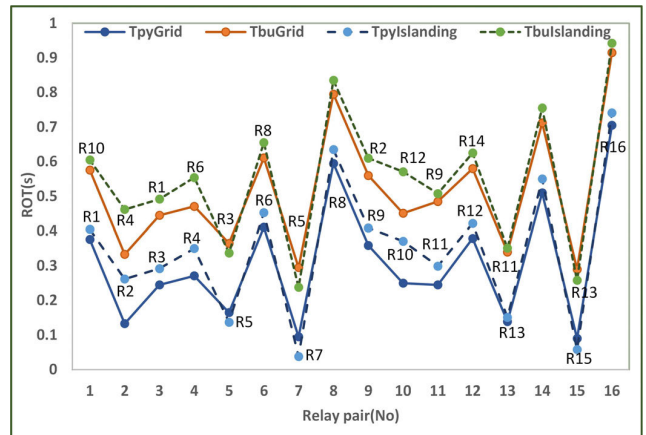


FIGURE 8. Coordination time between primary and backup relays pairs by considering user-defined characteristics for the 9-bus radial network.

10% subtransient reactance. The system bus voltage is taken as 12.47kV, and lines are 500m at length. The four synchronous based DGs are connected at buses, as shown in the figure. Each DG is rated with 5MVA capacity having 9.67% subtransient reactance. The DGs are connected with the system by 3.3/12.47kV step-up transformer with rating 10MVA and 5% subtransient reactance. Further, each line is protected with microprocessor-based directional overcurrent relays (DOCR) connected at the near-end and the far end of the line. In this case, a 400:5 current transformation (CT) ratio is taken for DOCR relay with their associated potential transformer (PT) rating 12.47kV/120 V. According to IEC 60909 short circuit studies, three-phase bolted faults are applied at nodes (F1-F8) that represents the location of the fault occurrence on the lines.

The simulation results of the relay coordination settings for the network different operating modes are presented in Table 2 and Table 3 with the specific value of the

TABLE 6. Optimal relay settings for 23-Bus Radial DN.

Scenario 1 (Grid Connected)							Scenario 2 (Islanding)					
Standard Characteristics			User-Defined Characteristics				Standard Characteristics		User-Defined Characteristics			
RELAYS	PSC	TMS	PSC	TMS	A	B	PSC	TMS	PSC	TMS	A	B
1	2.5	0.415	2.5	1.033	11.501	0.5898	1.8	0.2735	0.5	1.096	12.91	0.604
2	2.5	0.05	2.5	0.11	13.496	0.495	2.5	0.09	2.5	1.014	8.556	0.901
3	2	0.248	2	0.783	12.47	0.7093	1.3	0.2095	0.8	1.088	13.09	0.77
4	1.4	0.105	1.9	0.226	12.47	0.5451	1.1	0.1741	0.6	1.071	13.43	0.702
5	2.1	0.159	1.7	1.053	13.8	0.8954	1.2	0.1595	1.7	1.028	12.53	1
6	2	0.164	1	1.032	12.777	0.7123	1.3	0.2389	2	1.06	11.5	0.751
7	1	0.128	1.6	0.734	13.799	0.9999	0.7	0.1243	0.6	0.051	12.4	0.251
8	2.2	0.231	1.8	1.091	13.783	0.7023	1.5	0.3175	2	1.029	13.5	0.672
9	0.5	0.05	0.7	0.05	12.889	0.9967	0.5	0.05	0.6	0.62	12.12	0.999
10	2.3	0.326	2.5	1.1	11.8	0.5998	2.5	0.3895	2.5	1.095	12.5	0.653
11	0.5	0.05	0.5	0.05	12.905	0.9713	0.5	0.05	2.1	0.05	11.88	0.850
12	0.5	0.05	0.5	0.05	5.6785	0.6478	0.5	0.05	2.5	0.05	10.37	0.545
13	0.5	0.05	0.9	0.05	12.216	0.9962	0.5	0.05	2.4	0.05	12.65	0.477
14	2.4	0.326	1.5	1.046	13.78	0.5935	0.5	0.2734	2.1	0.479	12.96	0.55
15	1.3	0.235	1.5	1.035	13.51	0.7665	-	-	-	-	-	-
16	1.8	0.156	1.5	1.097	13.028	0.7834	-	-	-	-	-	-
17	0.5	0.05	0.5	0.05	12.93	0.9899	-	-	-	-	-	-
18	1.6	0.395	2.5	1.06	13.541	0.6063	1.7	0.2875	0.8	1.045	12.05	0.589
19	2.5	0.11	2.5	0.465	12.124	0.789	2.1	0.119	2.1	0.859	0.141	0.075
20	2.5	0.334	2.2	0.898	12.454	0.516	1.7	0.2486	2.5	1.07	13.13	0.683
21	1.6	0.222	2.5	1.07	13.246	0.7153	0.8	0.2412	2.2	1.066	8.898	0.578
22	2.5	0.245	1	1.091	12.424	0.5329	1.4	0.2147	1.2	1.081	12.47	0.656
23	2.3	0.257	1.2	1.052	13.562	0.5727	0.8	0.3217	2.5	1.087	11.03	0.573
24	1.6	0.190	2.2	1.084	11.641	0.7124	1.2	0.1546	2.4	0.678	11.72	0.719
25	2.2	0.318	1.2	1.081	13.78	0.5351	0.9	0.3606	2.5	1.092	10.35	0.513
26	2.18	0.101	1	1.073	13.351	0.8407	1.1	0.0978	2.5	0.342	10.28	0.804
27	2.4	0.349	2.5	1.078	13.671	0.6145	1.4	0.4121	2.2	1.069	12.48	0.531
28	0.5	0.05	1	1.033	13.111	0.9992	0.5	0.05	0.5	0.05	0.141	0.019
29	2.5	0.454	2.5	1.039	13.58	0.5101	1.8	0.4823	2.5	1.076	12.89	0.469
30	2.2	0.214	2	0.474	12.71	0.5159	2.4	0.2437	1.9	1.072	12.86	0.595
31	2.0	0.145	2	1.071	13.309	0.7617	2.5	0.1694	1.8	1.084	11.25	0.637
32	0.5	0.102	1.5	1.081	13.788	0.8722	-	-	-	-	-	-
33	0.5	0.05	0.5	0.05	0.1404	0.9068	-	-	-	-	-	-
O. F	12.0312 sec		8.3373 sec				12.9461 sec		9.9802 sec			

objective function. The optimal relay settings TMS and PCS obtain by the proposed technique SSA-LP demonstrate the performance and convergence of objective function (OF) compared to other established techniques in [27], [29]. It can be observed from the Tables, the user-defined characteristics (UDC) relay parameters performed better with the value of OF decrease from 5.443sec to 3.650sec in scenario 1. Meanwhile, for scenario 2, the solution converges from 5.859sec to 4.341sec. Hence, UDC results show better relay performance by quickly sensing fault in the network and rectifying in less time than the standard relay characteristics. Fig. 6 shows improvement in obtaining the relay settings for different network operating states using SSA_LP compared to the other hybrid techniques.

B. 23-BUS RADIAL DISTRIBUTION NETWORK

The second test system in this study is a practical system, 23-Bus Malaysian radial DN. The system is connected with a Grid capacity of 100MVA SC and X/R ratio of 6% [46]. The grid is connected to a bus through a 132kV/ 11kV transformer having a 10% subtransient reactance. The synchronous based DGs are considered with their maximum dispatch capacity of 2*1.82MVA and 1.86MVA and feed the system through 2MVA step-up transformer 3.3kV/11kV with 5% subtransient reactance. This system is provided with microprocessor-based directional and non-directional overcurrent relays, as shown in Fig. 7. The system contains different CT ratios for the relay currents because of different branch currents, as stated in Table 4.

TABLE 7. Comparison of relay operating times for scenario-1 (grid-connected) for 9-bus dn.

Fault Location	Relays		Standard Characteristics						User-Defined Characteristics			
			GA-LP [27]		CS-LP [29]		Proposed SSA LP		CS-LP [29]		Proposed SSA LP	
			Primary	Backup	Tp	Tb	Tp	Tb	Tp	Tb	Tp	Tb
F1	R1	R10	0.6972	1.33	0.5527	0.7527	0.505	0.705	0.2713	0.4713	0.376	0.576
	R2	R4	1.311	1.5143	0.6966	0.8966	0.296	0.495	0.3553	0.5553	0.133	0.333
	R3	R1	0.5183	0.7200	0.4396	0.6396	0.392	0.592	0.2844	0.4844	0.245	0.445
F2	R4	R6	1.4906	1.6922	0.8128	1.0128	0.495	0.695	0.3963	0.5963	0.271	0.471
	R5	R3	0.3345	0.5384	0.2916	0.4916	0.275	0.475	0.2233	0.4233	0.165	0.365
F3	R6	R8	1.666	2.9116	0.9016	1.1016	0.689	0.89	0.3851	0.5851	0.411	0.611
	R7	R5	0.1329	0.3484	0.1191	0.3191	0.090	0.300	0.1	0.3	0.095	0.295
F4	R8	R0	-	-	-	-	-	-	-	-	-	-
	R9	R2	0.6998	1.3617	0.557	0.757	0.496	0.696	0.263	0.463	0.359	0.560
F5	R10	R12	1.2873	2.353	0.6769	0.8769	0.284	0.485	0.3203	0.5203	0.250	0.451
	R11	R9	0.4896	0.7247	0.4349	0.6349	0.395	0.598	0.2351	0.4351	0.245	0.485
F6	R12	R14	2.113	2.3189	0.8205	1.0205	0.491	0.695	0.4265	0.6265	0.379	0.580
	R13	R11	0.3016	0.5103	0.3004	0.5004	0.276	0.475	0.206	0.406	0.139	0.340
F7	R14	R16	2.175	2.382	0.9499	1.1499	0.825	1.025	0.4996	0.6996	0.510	0.712
	R15	R13	0.1144	0.3188	0.1345	0.3345	0.084	0.285	0.1	0.3	0.090	0.290
F8	R16	0	-	-	-	-	-	-	-	-	-	
TOTAL OPERATING TIME (SECONDS)			13.331	19.024	7.688	10.4881	5.593	8.411	4.0662	6.866	3.668	6.514

TABLE 8. Comparison of relay operating times for scenario-2 (islanding) for 9-bus dn.

Fault Location	Relays		Standard Characteristics				User-Defined Characteristics			
			CS-LP [29]		Proposed SSA LP		CS-LP [29]		Proposed SSA LP	
			Primary	Backup	Tp	Tb	Tp	Tb	Tp	Tb
F1	R1	R10	0.5833	0.7833	0.521	0.722	0.3327	0.536	0.405	0.605
	R2	R4	0.7757	0.9757	0.535	0.736	0.5074	0.707	0.262	0.462
F2	R3	R1	0.4732	0.6732	0.401	0.601	0.3251	0.525	0.292	0.492
	R4	R6	0.8667	1.0667	0.668	0.870	0.5026	0.703	0.350	0.554
F3	R5	R3	0.3332	0.5332	0.249	0.45	0.2581	0.458	0.137	0.337
	R6	R8	0.948	1.4095	0.842	1.05	0.5001	1.174	0.453	0.655
F4	R7	R5	0.1374	0.3692	0.095	0.295	0.1002	0.338	0.050	0.250
	R8	-	-	-	-	-	-	-	-	
F5	R9	R2	0.6588	0.8597	0.623	0.823	0.4645	0.667	0.409	0.61
	R10	R12	0.6897	3.6154	0.514	0.715	0.4766	0.872	0.371	0.571
F6	R11	R9	0.4662	0.7459	0.421	0.621	0.3122	0.674	0.299	0.508
	R12	R14	3.4377	3.6381	0.643	0.645	0.7102	0.911	0.422	0.625
F7	R13	R11	0.3162	0.5162	0.290	0.490	0.2098	0.41	0.151	0.351
	R14	R16	3.3992	3.5998	0.787	0.989	0.7205	0.921	0.550	0.755
F8	R15	R13	0.1577	0.3574	0.138	0.339	0.1001	0.3	0.058	0.258
	R16	-	-	-	-	-	-	-	-	
TOTAL OPERATING TIME (SECONDS)			13.243	19.143	6.727	9.346	5.5201	9.195	4.209	7.033

The electrical boundaries of MG, as shown in Fig. 7, were obtained through mathematical modelling designed for restoring load during the islanded mode of operation with the capacity constraints of MG sources at buses 8 & 19. The restoration model is solved by using GUROBI solver in AMPL. The objective of the restoration model is to meet the highest possible load demand based on the generation and the load priority given to them, as mentioned in Table 5. The restoration scheme also utilizes the tie switches (if available) in the network to restore the loads

by considering minimum power loss. It should be noted that the objective function for the restoration model was taken from [47].

The test results of the proposed technique SSA-LP are presented in Table 6. The results present the optimal relay settings of TMS and PCS and the value of objective function obtained in grid-connected and off-grid modes with different relay characteristics. The proposed UDC settings converge the PCP in less time for MG, both operating scenarios compared to the standard relay characteristics. This new UDC can

TABLE 9. Operating time of relays for Scenario 1 and scenario 2 for 23-Bus Radial DN.

Fault Location	Relays		Scenario 1(Grid Connected)				Scenario 2 (Islanding)			
			Standard Characteristics		User-Defined Characteristics		Standard Characteristics		User-Defined Characteristics	
			TP	TB	TP	TB	TP	TB	TP	TB
F1	R1	R19	0.879	1.080	0.447	0.650	0.937	1.137	0.606	0.806
	R2	R4	0.298	0.500	0.269	0.471	0.327	0.527	0.297	0.500
F2	R3	R1	0.690	0.892	0.338	0.540	0.738	0.938	0.505	0.705
	R4	R6	0.415	0.615	0.367	0.567	0.528	0.730	0.408	0.610
F3	R5	R3	0.506	0.706	0.290	0.490	0.574	0.775	0.415	0.615
	R6	R8	0.583	0.785	0.408	0.611	0.698	0.899	0.523	0.723
F4	R7	R5	0.369	0.570	0.170	0.370	0.401	0.601	0.313	0.515
	R8	R10	0.708	0.909	0.582	0.795	0.890	1.090	0.669	0.870
F5	R9	R7	0.137	0.340	0.074	0.275	0.161	0.363	0.131	0.350
	R10	-	0.899	-	0.76	-	1.097	-	0.893	1.095
F6	R11	R10	0.087	0.290	0.050	0.250	0.088	0.288	0.057	0.260
F7	R12	R1	0.101	0.301	0.059	0.260	0.107	0.310	0.052	0.255
F8	R13	R1	0.085	0.285	0.057	0.265	0.098	0.300	0.063	0.265
F9	R14	R1	0.589	0.989	0.448	0.650	0.594	0.795	0.475	0.675
F10	R15	R14	0.435	0.635	0.292	0.492	-	-	-	-
F11	R16	R15	0.295	0.495	0.139	0.340	-	-	-	-
F12	R17	R16	0.100	0.310	0.061	0.261	-	-	-	-
F13	R18	R2	0.884	1.015	0.487	0.687	0.945	1.150	0.733	0.935
	R19	R21	0.403	0.603	0.308	0.509	0.417	0.617	0.355	0.555
F14	R20	R18	0.722	0.922	0.424	0.624	0.774	0.975	0.588	0.790
	R21	R23	0.560	0.765	0.417	0.617	0.606	0.806	0.525	0.725
F15	R22	R20	0.573	0.773	0.387	0.589	0.655	0.855	0.421	0.621
	R23	R25	0.673	0.873	0.514	0.715	0.783	0.983	0.663	0.865
F16	R24	R22	0.433	0.633	0.227	0.435	0.510	0.710	0.312	0.515
	R25	R27	0.799	0.901	0.613	0.815	0.938	1.140	0.789	0.995
F17	R26	R24	0.299	0.500	0.151	0.351	0.326	0.526	0.189	0.390
	R27	R29	0.946	1.150	0.717	0.915	1.086	1.295	0.937	1.140
F18	R28	R26	0.117	0.320	0.080	0.208	0.153	0.353	0.068	0.270
	R29	-	1.075	-	0.892	-	1.226	-	1.014	-
F19	R30	R28	0.454	0.655	0.375	0.575	0.715	0.915	0.508	0.710
F20	R31	R30	0.321	0.521	0.237	0.437	0.590	0.800	0.368	0.570
F21	R32	R31	0.207	0.407	0.139	0.340	-	-	-	-
F22	R33	R32	0.098	0.300	0.055	0.255	-	-	-	-
TOTAL OPERATING TIME (SECONDS)			15.740	20.040	10.834	15.359	16.962	19.878	12.877	17.325

provide faster and efficient relay operation for various types of faults that could be occurred in the network.

C. ANALYSIS OF RELAY OPERATING TIMES

This section discusses the coordination results of primary and backup relays for the fault current passing through them from different directions. It is to be noted that the relay performance is affected due to fault types (such as phase-phase faults or phase to ground faults) and fault resistance. Although these uncertainties can alter the magnitude without changing the fault direction. Therefore, in this study, a three-phase bolted fault current is assumed at the mid-point of lines on the 9-Bus, and 23-Bus radial DN as presented in Table 7 and Table 8. Furthermore, a comparison between the performance of standard relay characteristics and

proposed relay characteristics have been observed for the bidirectional faults in the system. The relay settings obtained by the hybrid technique has been verified on both test systems for the two grid operating scenarios, as mentioned in section IV.

In Scenario 1 for the 9-Bus network, the fault is considered at location F2, the operating time for R3 is **0.392sec**, and R4 is **0.495sec**, and their associated backup relay timings are R1 and R6 are **0.592 and 0.695** seconds. Moreover, considering UDC for the same scenario and fault location, all the relays operating time almost reduced to half. The primary relays R3 and R4 clear the fault in **0.245 & 0.271** sec, and their associated backup relays operating times are **0.445 & 0.471** seconds. From the results, it can be observed that the relays are properly coordinated in both scenarios; however,

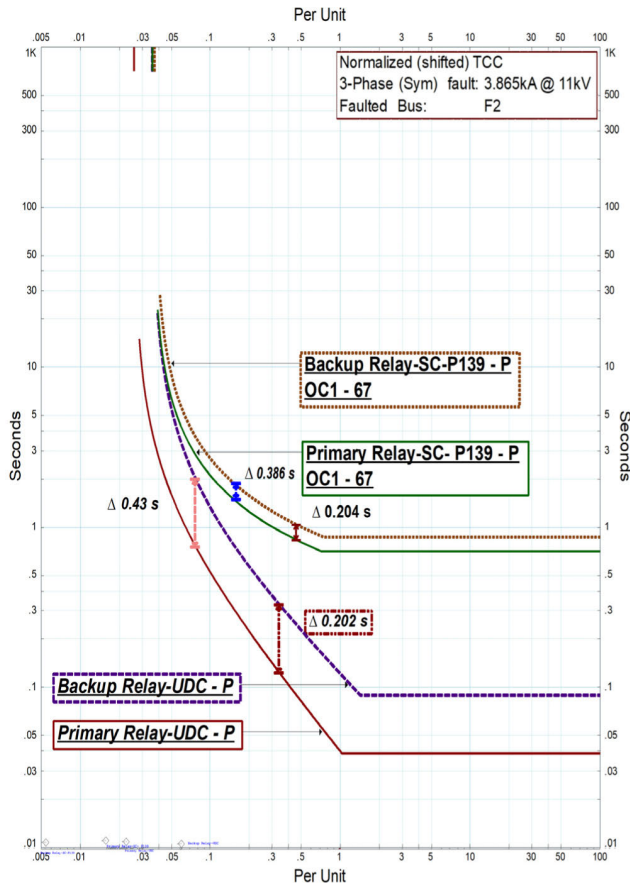


FIGURE 9. TCC comparison with a user-defined relay characteristic for the fault at location F_2 in a grid-connected mode.

the proposed characteristics decrease the overall operating time and provide a fast operation to clear the faults. For Scenario 2, if there could be any kind of change in the network topology, e.g., Islanding, the proposed algorithm presents better coordination results. In the islanded mode, the relay operating time increases due to a reduction in the fault levels; therefore, the relay coordination settings need to be updated accordingly. Table 7 and 8 presented the primary and their associated backup relay operating time.

The results show that the relays are properly coordinated and meeting the CTI constraint, which must be (≥ 200 msec). Moreover, to verify the updated relay coordination settings with the change in network topology, a three-phase fault is considered at location F_2 . The relay settings R_3 and R_4 clears the fault in **0.401 and 0.668** seconds, and their backup timings are set at **0.601 and 0.870** seconds, respectively. Similarly, by formulating the protection problem by considering UDC parameters. The operating time of R_3 and R_4 relays for the same fault F_2 is **0.292 and 0.350**secs, and their backup relays R_1 and R_6 are **0.492 and 0.554**secs, respectively. The remaining operating time of the relays for the fault at other lines in the different network operating scenarios are presented in Tables 7 and 8. Fig.8 depicts the improvement in the coordination time for 16 relay pairs by considering the

TABLE 10. optimal relay settings for state 1.

Relays	Standard Characteristics		User-Defined Characteristics			
	PCS	TMS	PCS	TMS	A	B
1	2.48	0.000	1.4	0.000	5.476	0.682
2	0.5	0.000	1.5	0.000	7.984	0.937
3	0.5	0.000	0.99	0.000	7.872	0.866
4	1.7	0.1276	1.1	0.1075	12.25	0.696
5	2.5	0.000	2.3	0.000	11.64	0.892
6	1.6	0.1671	1.3	0.1441	10.06	0.766
7	0.6	0.000	1.7	0.000	9.371	0.870
8	1.7	0.1905	1.6	0.1705	13.77	0.996
9	1.9	0.000	1.6	0.000	12.81	0.671
10	2.1	0.2095	1.8	0.1895	12.95	0.952
11	2.2	0.2913	1.7	0.2451	10.71	0.616
12	2.1	0.2959	2.1	0.2091	9.566	0.671
13	2.47	0.0500	0.6	0.0500	11.97	0.500
14	1.9	0.1300	0.5	0.0500	13.45	0.559
15	1.1	0.2193	1.4	0.1412	11.79	0.495
16	0.7	0.1951	1.1	0.1231	10.03	0.632
17	0.5	0.1453	1.3	0.1295	8.760	0.645
18	0.5	0.0500	0.5	0.0500	13.32	0.656
19	2.9	0.000	2.2	0.0000	11.16	0.161
20	2.6	0.000	1.4	0.0000	10.95	1.000
21	0.5	0.000	1.2	0.0000	10.43	0.870
22	2.8	0.000	0.9	0.0000	12.75	0.072
23	2.1	0.000	0.8	0.0000	7.710	0.021
24	2.4	0.000	2.4	0.0000	13.71	0.435
25	2.2	0.000	1.5	0.0000	11.96	0.113
26	0.5	0.0500	0.5	0.0500	13.02	0.855
27	1.1	0.000	2.3	0.0000	13.41	0.781
28	0.7	0.1081	0.5	0.1211	10.32	0.679
29	1.2	0.000	0.6	0.0000	13.22	0.992
30	1.1	0.1155	0.8	0.1571	7.550	0.699
31	1.6	0.1531	1.1	0.1091	9.345	0.515
32	1.1	0.0745	0.8	0.1191	9.330	0.951
33	1.8	0.1091	1.6	0.1490	6.390	0.876
34	1.1	0.0961	0.8	0.1558	8.230	0.601
35	1.0	0.0743	1.6	0.0891	13.22	0.472
36	0.5	0.0500	0.5	0.0500	13.67	0.653
37	2.1	0.2156	1.4	0.1891	13.18	0.712
38	2.2	0.3352	2.5	0.2541	11.82	0.783
O.F	8.2826 Sec		6.3472 Sec			

UDC, and the CTI for all relay pairs is consistently equal to or greater than 200msec for both operating modes of MG.

Table 9 presents the results of the relay operating time tested on 23-bus DN for both scenarios. For scenario 1 at-fault location F_2 , the operating time for R_3 is **0.690** sec, and R_4 is **0.415** sec, and their associated backup relay timings are R_1 and R_6 are **0.892 and 0.615** sec. Whereas the same fault scenario by considering UDC relays, the operating time gets decreases. The primary relays R_3 and R_4 clear the fault in **0.338 & 0.367** sec, and their backup operating timings are **0.540 & 0.567** sec. Fig. 9. shows a comparison between the time characteristic curve (TCC) for standard and UDC relay to clear the fault at the same location.

In scenario 2, when the MG operates in the islanded mode, the relay settings need to be updated according to the current network state. Therefore, the network restoration algorithm proposed in [47] is implemented to restore the critical and semi-critical load for the continuity of supply based on the available generation of DGs. The relay settings are also updated according to the restored network. The relay settings obtained during islanded mode are presented

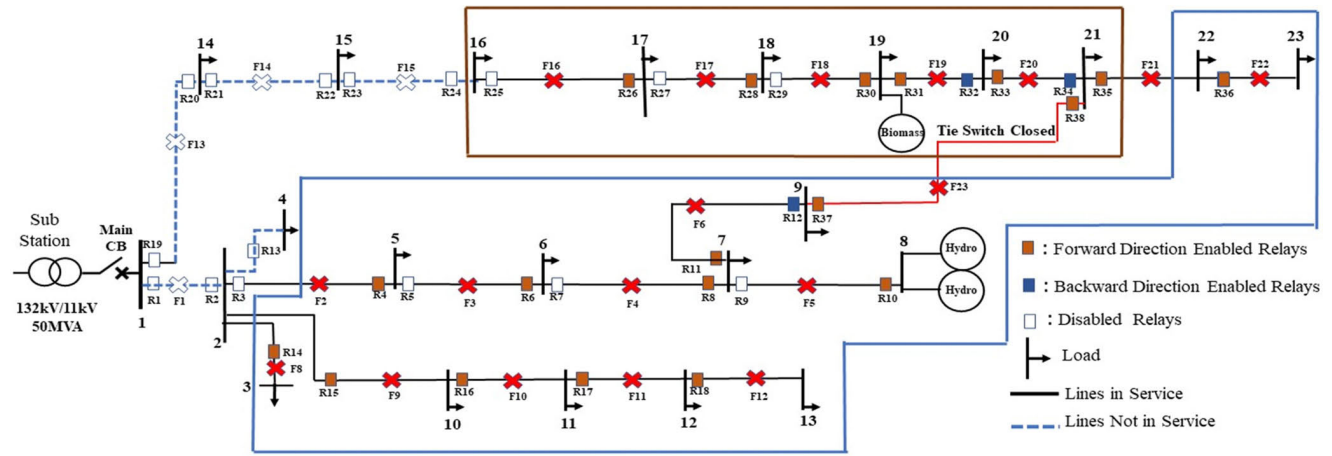


FIGURE 10. The layout of reconfigured 23-bus radial DN during Islanded Mode.

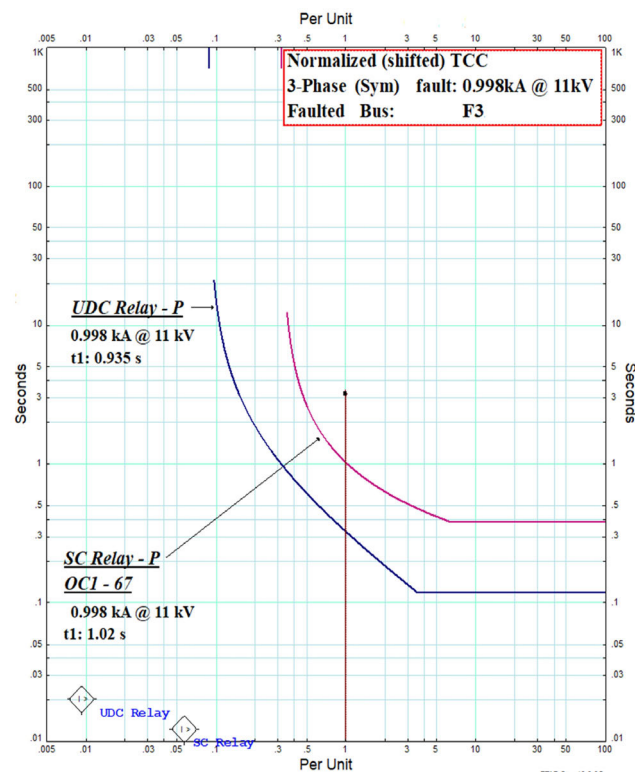


FIGURE 11. Comparison of relay characteristics during fault conditions.

in Table 6 by considering the standard and user-defined relay characteristics. In this scenario, the operating time for the relay increase because of a reduction in fault levels. Therefore, the relay settings need to be optimized accordingly and coordinated with their associated relay backup pairs, which must be (≥ 200 ms). Relay R₃ and R₄ operating times are **0.738 sec** and **0.528 sec**, respectively, and their backup timings are **0.938** and **0.730** secs, respectively. Similarly, in the case of **UDC** relay settings, the relay timing of R₃ and R₄ is **0.505** sec, and 0.408 sec with their backup relays R₁ and R₆

are **0.705** and **0.610** secs. The remaining operating time and coordination between relays for the faults at other lines are given in Table 9.

Table 9 shows the operating time for 35 relays and their coordination between primary and backup relays pairs. By comparing the results of the standard and proposed relay characteristics curve, the consideration of UDC for digital relays decreases the overall operating time from **15.740 secs** to **10.834 secs** for **scenario 1**. For **scenario 2**, it has been reduced from **16.962 secs** to **12.877 secs**. The results show the effectiveness of the proposed approach that the relays are properly coordinated and fulfil the CTI requirements without unnecessary tripping for the three-phase fault current that occurred in the two operating modes of MG based DN. It can also be depicted from the Fig. 9 that the proposed relay characteristics can maintain the coordination settings for the other types of phase faults due to the inverse nature of TCC. However, the proposed study can be further extended to obtain the relay settings for zero sequence faults including fault resistance.

D. RELAY COORDINATION SETTINGS FOR RECONFIGURED MG

In this section, the performance of the proposed hybrid optimization approach is tested during the reconfigured MG, especially in the case of an Islanded operating mode. Therefore, the protection settings need to be updated according to the topological change in the network.

For this scenario, two cases have been considered to obtain the relay settings.

State 1: Relay coordination settings for the reconfigured network subjected to pre-contingency faults.

State 2: Relay coordination settings for the reconfigured network subjected to post-contingency faults.

To verify the efficacy of the hybrid technique in reconfigured networks, the same 23-Bus Malaysian DN model is considered with a tie switch, as shown in Fig. 10.

TABLE 11. Relay operating time during state 1 condition.

Fault Location	Relays		Standard Characteristics		User-Defined Characteristics	
	Primary	Backup	Tp	Tb	Tp	Tb
F1	R1	-	-	-	-	-
	R2	-	-	-	-	-
F2	R3	-	-	-	-	-
	R4	R6	0.856	1.060	0.789	0.992
F3	R5	-	-	-	-	-
	R6	R8	1.023	1.231	0.935	1.136
F4	R7	-	-	-	-	-
	R8	R10	1.188	1.388	1.075	1.275
F5	R9	-	-	-	-	-
	R10	-	1.455	-	1.145	-
F6	R11	R10	1.368	1.569	0.952	1.152
	R12	R38	1.195	1.395	1.052	1.256
F7	R13	R4	0.145	0.351	0.128	0.328
F8	R14	R4	0.127	0.329	0.113	0.325
F9	R15	R4	0.719	0.919	0.615	0.819
F10	R16	R15	0.521	0.721	0.446	0.648
F11	R17	R16	0.329	0.529	0.247	0.454
F12	R18	R17	0.113	0.313	0.078	0.278
F13	R19	-	-	-	-	-
	R20	-	-	-	-	-
F14	R21	-	-	-	-	-
	R22	-	-	-	-	-
F15	R23	-	-	-	-	-
	R24	-	-	-	-	-
F16	R25	-	-	-	-	-
	R26	R28	0.135	0.338	0.085	0.285
F17	R27	-	-	-	-	-
	R28	R30	0.331	0.535	0.245	0.445
F18	R29	-	-	-	-	-
	R30	R32	0.515	0.715	0.415	0.621
F19	R31	-	1.686	-	1.572	-
	R32	R34	0.691	0.895	0.615	0.823
F20	R33	R31	1.532	1.735	1.397	1.599
	R34	R37	0.878	1.178	0.795	0.995
F21	R35	R33	0.253	0.455	0.225	0.430
F22	R36	R35	0.096	0.300	0.083	0.285
F23	R37	R11	1.166	1.366	0.979	1.181
	R38	R33	1.368	1.589	1.242	1.451
Total Operating Time (Seconds)			17.690	18.914	15.277	16.778

As discussed in Section V-B, the restoration model is implemented to restore the loads when the tie switch is closed during the MG islanded mode of operation. Therefore, the relay settings must be updated according to the new structure of DN to avoid unnecessary tripping during pre and post-contingency fault scenarios. The relay settings for state 1 are given in Table 10.

The results obtained by the proposed technique indicate the proper coordination between relays has achieved and complies with the coordination constraints for bidirectional faults, as presented in Table 11. The relays provided with

TABLE 12. Optimized relay settings for state 2.

Relays	Standard Characteristics			User-Defined Characteristics			
	PCS	TMS		PCS	TMS	A	B
1	1.97	-		1.4	-	5.47	0.68
2	0.52	-		1.5	-	12.24	0.43
3	2.48	-		2	-	13.56	0.95
4	1.99	-		0.6	-	12.61	0.2
5	0.58	-		1.6	-	11.72	0.16
6	0.51	-		1.3	-	10.52	0.81
7	1	-		1.4	-	11.25	0.28
8	0.5	0.05		0.5	0.05	13.12	0.99
9	2.39	-		0.6	-	3.27	0.42
10	2.5	0.520		0.8	0.152	11.15	0.65
11	2.4	0.285		1.9	0.189	10.6	0.52
12	1.9	0.295		1.5	0.175	10.91	0.92
13	0.5	-		0.9	-	13.76	0.11
14	2.5	-		0.6	-	12.55	0.61
15	0.6	-		2	-	9.68	0.13
16	1.6	-		2.4	-	10.55	0.38
17	1.3	-		1.5	-	8.73	0.37
18	2.5	-		1.8	-	12.26	0.73
19	0.7	-		1.7	-	10.2	0.21
20	2.2	-		2.3	-	11.66	0.53
21	0.8	-		1.2	-	10.43	0.87
22	2.1	-		0.93	-	12.75	0.07
23	1.1	-		0.82	-	7.71	0.02
24	0.5	0.05		0.7	0.05	7.35	0.99
25	0.78	-		2	-	9.84	0.34
26	1.1	0.0791		0.9	0.074	10.39	0.67
27	1.54	-		1.3	-	6.63	0.4
28	1.5	0.1046		1.1	0.103	13.61	0.76
29	2.11	-		1.6	-	8.33	0.67
30	1.5	0.125		1.2	0.133	12.04	0.41
31	1.4	0.152		0.6	0.131	13.61	0.66
32	0.8	0.131		0.8	0.155	13.3	0.85
33	1.3	0.148		0.5	0.102	12.51	0.56
34	1.1	0.114		0.9	0.160	10.49	0.69
35	2.5	0.117		2.4	1.033	10.58	0.75
36	0.5	0.05		0.5	0.05	9.17	0.97
37	2.4	0.245		1.6	0.174	11.76	0.51
38	2.5	0.174		1.5	0.211	6.04	0.57
O.F	4.8641 Sec			3.582 Sec			

UDC can perform faster with better coordination than the standard relay characteristics. Fig.11 shows the performance standard and proposed characteristic for the fault created at location **F₃**. It can be observed from the figure that the proposed characteristic provides a more flexible way to sense the inverse time fault currents compared to standard characteristics.

The same fault **F₃** is assumed as a permanent fault and cleared by the associated protection scheme in the previous case. Hence, the MG operating status changes accordingly, as shown in Fig. 12. The circuit shows the enabled relays that need to be updated according to the network's new operating state to sense the faults during post contingency scenarios. Table 12 shows the optimal settings of relay parameters for the faults during the post contingency condition. Table 13 illustrates the operating time of primary and backup relays to detect the faults and send the trip command to their associated circuit breaker to clear the fault in the shortest possible time. The results indicate that the relays are properly coordinated and comply with the coordination requirement during post contingency faults. Hence, the proposed approach

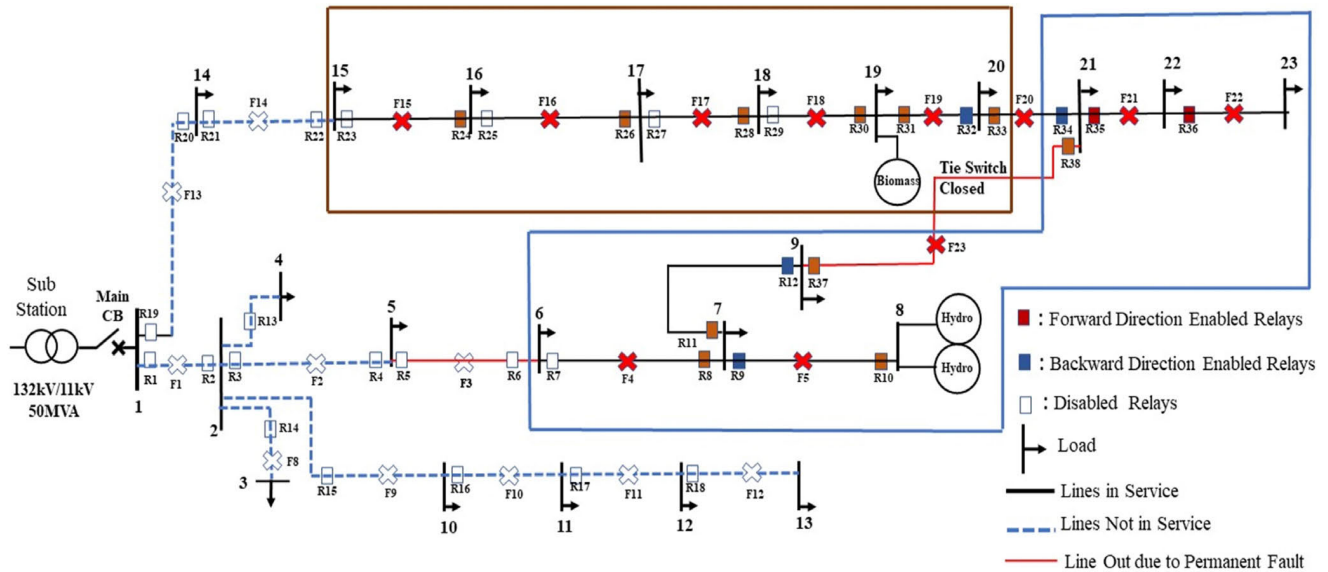


FIGURE 12. The layout of the reconfigured model after a permanent fault in 23-bus radial DN during Islanded Mode.

TABLE 13. Relays operating time for state 2 condition.

Fault Location	Relays		Standard Characteristics		User-Defined Characteristics	
	Primary	Backup	Tp	Tb	Tp	Tb
F1	R1	R4	-	-	-	-
F2	R3	R6	-	-	-	-
F3	R5	R8	-	-	-	-
F4	R7	R10	0.105	0.315	0.076	0.276
F5	R9	-	-	-	-	-
F6	R11	R10	1.295	1.499	1.214	1.42
F8	R13	R4	-	-	-	-
F9	R14	R4	-	-	-	-
F10	R15	R4	-	-	-	-
F11	R16	R15	-	-	-	-
F12	R17	R16	-	-	-	-
F13	R18	R17	-	-	-	-
F14	R19	-	-	-	-	-
F15	R20	-	-	-	-	-
F16	R21	-	-	-	-	-
F17	R22	-	-	-	-	-
F18	R23	-	-	-	-	-
F19	R24	-	0.117	0.317	0.0313	0.236
F21	R25	-	-	-	-	-
F23	R26	R28	0.312	0.512	0.215	0.421
F25	R27	-	-	-	-	-
F26	R28	R30	0.496	0.705	0.418	0.619
F27	R29	-	-	-	-	-
F27	R30	R32	0.668	0.878	0.582	0.791
F27	R31	0	1.299	-	0.932	-
F27	R32	R34	0.853	1.063	0.754	0.954
F27	R33	R31	1.195	1.401	0.749	0.949
F27	R34	R37	1.034	1.244	0.933	1.135
F27	R35	-	0.273	0.475	0.231	0.432
F27	R36	-	0.097	0.299	0.05	0.25
F27	R37	R11	1.195	1.405	1.085	1.295
F27	R38	R33	1.068	1.281	0.56	0.765
Total Operating Time (Seconds)			12.291	12.494	9.533	10.108

shows the desirable performance to minimize the operating time of relays for pre- and post-fault contingency in a reconfigured MG when operating in an islanded mode.

The results show the efficient performance of the hybrid optimization technique that provides a better result and fast convergence to solve the PCP in two stages to obtain the optimal values of relay settings. Moreover, by investigating the UDC results with the standard characteristics curve, the proposed characteristics reduce relay operating time by adjusting the relay constants A & B along with TMS and PCS. However, for large interconnected DN where the coordination problem (PCP) gets complex and the relay operating time increases, a multi-objective optimization [44] approach can be utilized to obtain accurate optimal relay settings considering user-defined characteristics. Also, to detect high impedance faults in the presence of inverter-based DGs, the use of dual voltage and current based time characteristic curve can be proposed to overcome the fault detection scenarios compared to conventional protection techniques.

VI. CONCLUSION

The work aims to mitigate the potential detrimental impacts of protection failure in an MG interconnected distribution network for the On/Off-grid operating modes. This paper proposes a two-stage hybrid optimization SSA-LP algorithm for optimal protection coordination scheme in a radially integrated distribution network. The first stage of the algorithm randomly explores the search space and optimizes the relay coordination parameters while complying with the constraints to avoid local solutions. A hybrid technique is implemented in the second stage to linearize the protection coordination problem and find the global solution and hence improve the accuracy of the relay coordination, according to CTI constraint. A user-defined characteristic for the over-current relays proposed in this work provides optimal relay coordination and has successfully reduced the total operating time of the relays for the faults that might occur in the

grid-connected and islanded mode of operations. This paper has also presented and discussed the coordination of relays in the reconfigured MG during a standalone operation where the protection settings need to be optimally changed according to the network layout. In this regard, the SSA-LP technique re-estimates the relay operating parameters and optimizes the protection settings according to the reconfigured network. The results confirmed the superiority of the proposed technique against other hybrid techniques in improving the solution quality and reducing the computational burden in determining the relay settings for dynamic operating modes of a network. In addition, the proposed technique provides optimal relay coordination for both pre-and post-contingency fault scenarios.

REFERENCES

- [1] L. Che, M. E. Khodayar, and M. Shahidehpour, "Adaptive protection system for microgrids: Protection practices of a functional microgrid system," *IEEE Electr. Mag.*, vol. 2, no. 1, pp. 66–80, Mar. 2014, doi: [10.1109/MELE.2013.2297031](https://doi.org/10.1109/MELE.2013.2297031).
- [2] A. Pathirana, A. Rajapakse, and N. Perera, "Development of a hybrid protection scheme for active distribution systems using polarities of current transients," *Electr. Power Syst. Res.*, vol. 152, pp. 377–389, Nov. 2017, doi: [10.1016/j.epsr.2017.07.022](https://doi.org/10.1016/j.epsr.2017.07.022).
- [3] H. F. Habib, A. A. S. Mohamed, M. El Hariri, and O. A. Mohammed, "Utilizing supercapacitors for resiliency enhancements and adaptive micro-grid protection against communication failures," *Electr. Power Syst. Res.*, vol. 145, pp. 223–233, Apr. 2017, doi: [10.1016/j.epsr.2016.12.027](https://doi.org/10.1016/j.epsr.2016.12.027).
- [4] T. N. Boutsika and S. A. Papathanassiou, "Short-circuit calculations in networks with distributed generation," *Electr. Power Syst. Res.*, vol. 78, no. 7, pp. 1181–1191, Jul. 2008, doi: [10.1016/j.epsr.2007.10.003](https://doi.org/10.1016/j.epsr.2007.10.003).
- [5] B. J. Brearley and R. R. Prabu, "A review on issues and approaches for microgrid protection," *Renew. Sustain. Energy Rev.*, vol. 67, pp. 988–997, Jan. 2017, doi: [10.1016/j.rser.2016.09.047](https://doi.org/10.1016/j.rser.2016.09.047).
- [6] I. Tristiu, C. Bulac, S. Costinas, L. Toma, A. Mandis, and T. Zabava, "A new and efficient algorithm for short-circuit calculation in distribution networks with distributed generation," in *Proc. 9th Int. Symp. Adv. Topics Electr. Eng. (ATEE)*, May 2015, pp. 816–821.
- [7] H. Margossian, J. Sachau, and G. Deconinck, "Short circuit calculation in networks with a high share of inverter based distributed generation," in *Proc. IEEE 5th Int. Symp. Power Electron. Distrib. Gener. Syst. (PEDG)*, Jun. 2014, pp. 1–5.
- [8] P. T. Manditereza and R. Bansal, "Renewable distributed generation: The hidden challenges—A review from the protection perspective," *Renew. Sustain. Energy Rev.*, vol. 58, pp. 1457–1465, May 2016, doi: [10.1016/j.rser.2015.12.276](https://doi.org/10.1016/j.rser.2015.12.276).
- [9] M. Norshahrani, H. Mokhlis, A. A. Bakar, J. Jamian, and S. Sukumar, "Progress on protection strategies to mitigate the impact of renewable distributed generation on distribution systems," *Energies*, vol. 10, no. 11, p. 1864, Nov. 2017.
- [10] V. Telukunta, J. Pradhan, A. Agrawal, M. Singh, and S. G. Srivani, "Protection challenges under bulk penetration of renewable energy resources in power systems: A review," *CSEE J. Power Energy Syst.*, vol. 3, no. 4, pp. 365–379, Dec. 2017, doi: [10.17775/CSEEJPES.2017.00030](https://doi.org/10.17775/CSEEJPES.2017.00030).
- [11] S. Katyara, L. Staszewski, and Z. Leonowicz, "Protection coordination of properly sized and placed distributed generations—methods, applications and future scope," *Energies*, vol. 11, no. 10, p. 2672, 2018.
- [12] M. N. Alam, B. Das, and V. Pant, "A comparative study of metaheuristic optimization approaches for directional overcurrent relays coordination," *Electr. Power Syst. Res.*, vol. 128, pp. 39–52, Nov. 2015, doi: [10.1016/j.epsr.2015.06.018](https://doi.org/10.1016/j.epsr.2015.06.018).
- [13] F. Coffele, C. Booth, and A. Dysko, "An adaptive overcurrent protection scheme for distribution networks," *IEEE Trans. Power Del.*, vol. 30, no. 2, pp. 561–568, Apr. 2015, doi: [10.1109/TPWRD.2013.2294879](https://doi.org/10.1109/TPWRD.2013.2294879).
- [14] P. H. A. Barra, D. V. Coury, and R. A. S. Fernandes, "A survey on adaptive protection of microgrids and distribution systems with distributed generators," *Renew. Sustain. Energy Rev.*, vol. 118, Feb. 2020, Art. no. 109524, doi: [10.1016/j.rser.2019.109524](https://doi.org/10.1016/j.rser.2019.109524).
- [15] H. C. Kılıçkiran, İ. Şengör, H. Akdemir, B. Kekezoğlu, O. Erdinç, and N. G. Paterakis, "Power system protection with digital overcurrent relays: A review of non-standard characteristics," *Electr. Power Syst. Res.*, vol. 164, pp. 89–102, Nov. 2018, doi: [10.1016/j.epsr.2018.07.008](https://doi.org/10.1016/j.epsr.2018.07.008).
- [16] C. A. C. Salazar, A. C. Enríquez, and S. E. Schaeffer, "Directional overcurrent relay coordination considering non-standardized time curves," *Electr. Power Syst. Res.*, vol. 122, pp. 42–49, May 2015, doi: [10.1016/j.epsr.2014.12.018](https://doi.org/10.1016/j.epsr.2014.12.018).
- [17] H. M. Sharaf, H. H. Zeineldin, D. K. Ibrahim, and E. E.-D.-A. El-Zahab, "A proposed coordination strategy for meshed distribution systems with DG considering user-defined characteristics of directional inverse time overcurrent relays," *Int. J. Electr. Power Energy Syst.*, vol. 65, pp. 49–58, Feb. 2015, doi: [10.1016/j.ijepes.2014.09.028](https://doi.org/10.1016/j.ijepes.2014.09.028).
- [18] H. Kılıçkiran, H. Akdemir, İ. Şengör, B. Kekezoğlu, and N. Paterakis, "A non-standard characteristic based protection scheme for distribution networks," *Energies*, vol. 11, no. 5, p. 1241, May 2018.
- [19] A. Y. Abdelaziz, H. Talaat, A. Nousseir, and A. A. Hajjar, "An adaptive protection scheme for optimal coordination of overcurrent relays," *Electr. Power Syst. Res.*, vol. 61, no. 1, pp. 1–9, 2002, doi: [10.1016/S0378-7796\(01\)00176-6](https://doi.org/10.1016/S0378-7796(01)00176-6).
- [20] T. Amraee, "Coordination of directional overcurrent relays using seeker algorithm," *IEEE Trans. Power Del.*, vol. 27, no. 3, pp. 1415–1422, Jul. 2012, doi: [10.1109/TPWRD.2012.2190107](https://doi.org/10.1109/TPWRD.2012.2190107).
- [21] H. A. Abyaneh, M. Al-Dabbagh, H. K. Karegar, S. H. H. Sadeghi, and R. A. J. Khan, "A new optimal approach for coordination of overcurrent relays in interconnected power systems," *IEEE Trans. Power Del.*, vol. 18, no. 2, pp. 430–435, Apr. 2003, doi: [10.1109/TPWRD.2002.803754](https://doi.org/10.1109/TPWRD.2002.803754).
- [22] M. M. Mansour, S. F. Mekhamer, and N. El-Kharbawe, "A modified particle swarm optimizer for the coordination of directional overcurrent relays," *IEEE Trans. Power Del.*, vol. 22, no. 3, pp. 1400–1410, Jul. 2007, doi: [10.1109/TPWRD.2007.899259](https://doi.org/10.1109/TPWRD.2007.899259).
- [23] M. Singh, B. K. Panigrahi, and A. R. Abhyankar, "Optimal coordination of directional over-current relays using teaching learning-based optimization (TLBO) algorithm," *Int. J. Electr. Power Energy Syst.*, vol. 50, pp. 33–41, Sep. 2013, doi: [10.1016/j.ijepes.2013.02.011](https://doi.org/10.1016/j.ijepes.2013.02.011).
- [24] N. Hussain, M. Nasir, J. C. Vasquez, and J. M. Guerrero, "Recent developments and challenges on AC microgrids fault detection and protection systems—A review," *Energies*, vol. 13, no. 9, p. 2149, May 2020, doi: [10.3390/en13092149](https://doi.org/10.3390/en13092149).
- [25] M. N. A. Rahim, H. Mokhlis, A. H. A. Bakar, M. T. Rahman, O. Badran, and N. N. Mansor, "Protection coordination toward optimal network reconfiguration and DG sizing," *IEEE Access*, vol. 7, pp. 163700–163718, 2019, doi: [10.1109/ACCESS.2019.2952652](https://doi.org/10.1109/ACCESS.2019.2952652).
- [26] F. A. Albasri, A. R. Alroomi, and J. H. Talaq, "Optimal coordination of directional overcurrent relays using biogeography-based optimization algorithms," *IEEE Trans. Power Del.*, vol. 30, no. 4, pp. 1810–1820, Aug. 2015, doi: [10.1109/TPWRD.2015.2406114](https://doi.org/10.1109/TPWRD.2015.2406114).
- [27] K. A. Saleh, H. H. Zeineldin, and E. F. El-Saadany, "Optimal protection coordination for microgrids considering n – 1 contingency," *IEEE Trans. Ind. Informat.*, vol. 13, no. 5, pp. 2270–2278, Oct. 2017, doi: [10.1109/TII.2017.2682101](https://doi.org/10.1109/TII.2017.2682101).
- [28] V. N. Rajput and K. S. Pandya, "A hybrid improved harmony search algorithm-nonlinear programming approach for optimal coordination of directional overcurrent relays including characteristic selection," *Int. J. Power Energy Convers.*, vol. 9, no. 3, pp. 228–253, 2018, doi: [10.1504/IJPEC.2018.092688](https://doi.org/10.1504/IJPEC.2018.092688).
- [29] M. Shabani and A. Karimi, "A robust approach for coordination of directional overcurrent relays in active radial and meshed distribution networks considering uncertainties," *Int. Trans. Electr. Energy Syst.*, vol. 28, no. 5, p. e2532, May 2018, doi: [10.1002/etep.2532](https://doi.org/10.1002/etep.2532).
- [30] A. Yazdaninejadi, S. Golshannavaz, D. Nazarpour, S. Teimourzadeh, and F. Aminifar, "Dual-setting directional overcurrent relays for protecting automated distribution networks," *IEEE Trans. Ind. Informat.*, vol. 15, no. 2, pp. 730–740, Feb. 2019, doi: [10.1109/TII.2018.2821175](https://doi.org/10.1109/TII.2018.2821175).
- [31] A. Yazdaninejadi and S. Golshannavaz, "Robust protection for active distribution networks with islanding capability: An innovative and simple cost-effective logic for increasing fault currents virtually," *Int. J. Electr. Power Energy Syst.*, vol. 118, Jun. 2020, Art. no. 105773, doi: [10.1016/j.ijepes.2019.105773](https://doi.org/10.1016/j.ijepes.2019.105773).
- [32] X. Wang and X. Li, "Fault recovery of micro-grid based on network reconfiguration," in *Proc. Asia-Pacific Power Energy Eng. Conf.*, Mar. 2012, pp. 1–4.

- [33] B. P. Bhattarai, B. Bak-Jensen, S. Chaudhary, and J. R. Pillai, "An adaptive overcurrent protection in smart distribution grid," in *Proc. IEEE Eindhoven PowerTech*, Jun. 2015, pp. 1–6.
- [34] T. Gangwar and S. Sarangi, "Adaptive relay setting for distribution system during reconfiguration," in *Proc. 14th IEEE India Council Int. Conf. (INDICON)*, Dec. 2017, pp. 1–6.
- [35] J. Keller and B. Kroposki, "Understanding fault characteristics of inverter-based distributed energy resources," Nat. Renew. Energy Lab. (NREL), Golden, CO, USA, Tech. Rep. NREL/TP-550-46698, 2010.
- [36] T. S. Ustun, C. Ozansoy, and A. Ustun, "Fault current coefficient and time delay assignment for microgrid protection system with central protection unit," *IEEE Trans. Power Syst.*, vol. 28, no. 2, pp. 598–606, May 2013, doi: [10.1109/TPWRS.2012.2214489](https://doi.org/10.1109/TPWRS.2012.2214489).
- [37] A. A. Memon and K. Kauhaniemi, "A critical review of AC microgrid protection issues and available solutions," *Electr. Power Syst. Res.*, vol. 129, pp. 23–31, Dec. 2015, doi: [10.1016/j.epsr.2015.07.006](https://doi.org/10.1016/j.epsr.2015.07.006).
- [38] V. A. Papaspiliotopoulos, G. N. Korres, V. A. Kleftakis, and N. D. Hatziaargyriou, "Hardware-in-the-loop design and optimal setting of adaptive protection schemes for distribution systems with distributed generation," *IEEE Trans. Power Del.*, vol. 32, no. 1, pp. 393–400, Feb. 2017, doi: [10.1109/TPWRD.2015.2509784](https://doi.org/10.1109/TPWRD.2015.2509784).
- [39] A. H. A. Bakar, B. Ooi, P. Govindasamy, C. Tan, H. A. Illias, and H. Mokhlis, "Directional overcurrent and earth-fault protections for a biomass microgrid system in Malaysia," *Int. J. Electr. Power Energy Syst.*, vol. 55, pp. 581–591, Feb. 2014, doi: [10.1016/j.ijepes.2013.10.004](https://doi.org/10.1016/j.ijepes.2013.10.004).
- [40] *Electrical Relays—Part 3: Single Input Energizing Quantity Measuring Relays With Dependent or Independent Time*, IEC Standard 60255-3, 1989.
- [41] M. Geidl, *Protection of Power Systems With Distributed Generation: State of the Art*. Zürich, Switzerland: Eidgenössische Technische Hochschule Zürich, EEH Power Systems, 2005.
- [42] S. H. Horowitz and A. G. Phadke, *Power System Relaying*, 4th ed. Hoboken, NJ, USA: Wiley, 2014.
- [43] D. Durand and D. Pieniazek, "Overcurrent protection & coordination for industrial applications," in *Proc. Ind. Appl. Soc. Annu. Meeting*, 2010, pp. 1–131.
- [44] S. Mirjalili, A. H. Gandomi, S. Z. Mirjalili, S. Saremi, H. Faris, and S. M. Mirjalili, "Salp swarm algorithm: A bio-inspired optimizer for engineering design problems," *Adv. Eng. Softw.*, vol. 114, pp. 163–191, Dec. 2017.
- [45] E. P. Dick and A. Narang, "Canadian urban benchmark distribution systems," CANMET Energy Technol. Centre-Varenes, Varenes, QC, Canada, Tech. Rep. CETC-Varenes 2005-121 (TR), 2005.
- [46] J. A. Laghari, H. Mokhlis, M. Karimi, A. H. A. Bakar, and H. Mohamad, "A new under-frequency load shedding technique based on combination of fixed and random priority of loads for smart grid applications," *IEEE Trans. Power Syst.*, vol. 30, no. 5, pp. 2507–2515, Sep. 2015, doi: [10.1109/TPWRS.2014.2360520](https://doi.org/10.1109/TPWRS.2014.2360520).
- [47] A. Arif and Z. Wang, "Networked microgrids for service restoration in resilient distribution systems," *IET Gener., Transmiss. Distrib.*, vol. 11, no. 14, pp. 3612–3619, Sep. 2017, doi: [10.1049/iet-gtd.2017.0380](https://doi.org/10.1049/iet-gtd.2017.0380).



MAHMOUD MOGHAVVEMI received the B.Sc. degree in electronics from the State University of New York at Buffalo, Buffalo, NY, USA, the M.Sc. degree in electrical engineering from the University of Bridgeport, Bridgeport, CT, USA, and the Ph.D. degree in electrical engineering from the University of Malaya, Kuala Lumpur, Malaysia. He was a Test and Design Engineer at CTI Electronics, Fairfield CT, USA, and the Director of the Informatics School of Engineering, Kuala Lumpur Malaysia. He joined the Department of Electrical Engineering, University of Malaya, where he is currently serving as a Full Professor. He is a reviewer for several distinguished journals in his field of expertise. He is the Founder and currently the Director of the Centre for Research in Applied Electronics, University of Malaya. His contributions to the scientific community are evident by more than 30 patents and more than 250 refereed journals and conference papers.



HAZLIE MOKHLIS (Senior Member, IEEE) received the B.E. degree in electrical engineering and the M.Eng.Sc. degree from the University of Malaya (UM), Malaysia, in 1999 and 2002, respectively, and the Ph.D. degree from the University of Manchester, U.K., in 2009. He is currently a Professor with the Department of Electrical Engineering, UM. He is also an Associate Member of the UM Power Energy Dedicated Advanced Research Centre (UMPEDAC). His research interests are distribution automation and power system protection.



NURULAFIQAH NADZIRAH MANSOR (Member, IEEE) received the B.Eng. degree from Vanderbilt University, USA, the M.Eng. degree in power system engineering from the University of Malaya, Malaysia, and the Ph.D. degree from The University of Manchester, U.K., in 2008, 2013, and 2018, respectively. From 2008 to 2014, she worked as a Process Engineer with Texas Instruments (M) Sdn. Bhd. She is currently a Senior Lecturer with the University of Malaya, Malaysia. Her research interests include distribution system modeling and optimization, distribution system planning and operation, integration of renewable energy, and smart grid.



HAROON FAROOQ received the Ph.D. degree in electrical engineering from Glasgow Caledonian University, U.K., in 2012. He is currently an Assistant Professor with the Electrical Engineering Department (RCET, Gujranwala), University of Engineering and Technology, Lahore, Pakistan. His research interests include power system quality, renewable energy systems, electric vehicles, and demand side management.



ALIREZA POURDARYAEI received the bachelor's degree in electrical and electronic engineering from Hormozgan University, Iran, in 2010, the M.Eng.Sc. degree in industrial electronic and control and the Ph.D. degree in power system from the University of Malaysia (UM), in 2014 and 2020, respectively. His current research interests include distribution automation, artificial intelligence (AI), energy management, and forecasting.



MUHAMMAD USAMA received the B.Sc. degree in electrical engineering from the University of Central Punjab Lahore, Pakistan, in 2012, and the M.Sc. degree in electrical engineering from the University of Engineering & Technology (UET) Lahore, Pakistan, in 2017. He is currently pursuing the Ph.D. degree in protection of smart distribution networks with the University of Malaya (UM). His current research interests include power system analysis and stability, smart distribution networks, and power system protection.